



Ethyl 2-(4-methoxyphenyl)-6-oxa-3-azabicyclo-[3.1.0]hexane-3-carboxylate: crystal structure and Hirshfeld analysis

Julio Zukerman-Schpector,^{a*} Fabricia H. Sugiyama,^a Ariel L. L. Garcia,^b Carlos Roque D. Correia,^b Mukesh M. Jotani^c and Edward R. T. Tiekink^{d‡}

Received 30 June 2017

Accepted 5 July 2017

Edited by W. T. A. Harrison, University of Aberdeen, Scotland

‡ Additional correspondence author, e-mail: edwardt@sunway.edu.my.

Keywords: crystal structure; pyrrolidyl; epoxide; Hirshfeld surface analysis.

CCDC reference: 1560463

Supporting information: this article has supporting information at journals.iucr.org/e

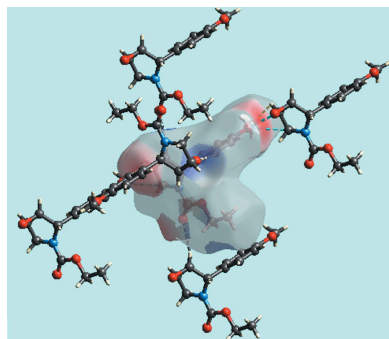
^aDepartamento de Química, Universidade Federal de São Carlos, 13565-905 São Carlos, São Paulo, Brazil, ^bInstituto de Química, Universidade Estadual de Campinas, UNICAMP, CP 6154, 13084-971, Campinas, São Paulo, Brazil, ^cDepartment of Physics, Bhavan's Sheth R. A. College of Science, Ahmedabad, Gujarat 380001, India, and ^dCentre for Crystalline Materials, School of Science and Technology, Sunway University, 47500 Bandar Sunway, Selangor Darul Ehsan, Malaysia. *Correspondence e-mail: julio@power.ufscar.br

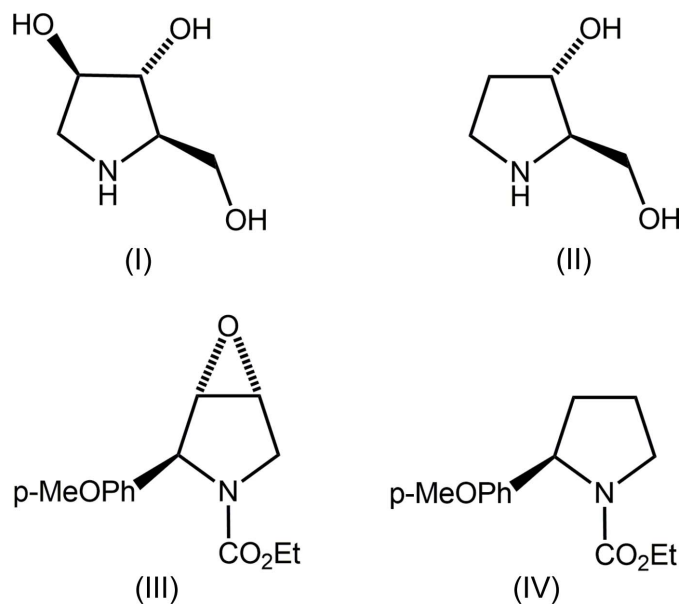
The title compound, C₁₄H₁₇NO₄, features an epoxide-O atom fused to a pyrrolidyl ring, the latter having an envelope conformation with the N atom being the flap. The 4-methoxyphenyl group is orthogonal to [dihedral angle = 85.02 (6)°] and lies to the opposite side of the five-membered ring to the epoxide O atom, while the N-bound ethyl ester group (r.m.s. deviation of the five fitted atoms = 0.0187 Å) is twisted with respect to the ring [dihedral angle = 17.23 (9)°]. The most prominent interactions in the crystal are of the type methine-C—H···O(carbonyl) and these lead to the formation of linear supramolecular chains along the *c* axis; weak benzene-C—H···O(epoxide) and methine-C—H···O(methoxy) interactions connect these into a three-dimensional architecture. The analysis of the Hirshfeld surface confirms the presence of C—H···O interactions in the crystal, but also the dominance of H···H dispersion contacts.

1. Chemical context

α -Glucosidase inhibitors have shown potential for the treatment of several health conditions such as cystic fibrosis, diabetes, influenza and cancer. In this context, a thorough patent review on α -glucosidase inhibitors was published recently (Brás *et al.*, 2014). Among α -glucosidase inhibitors are a series of natural products including aminocyclitols (I) and (II); see Scheme 1. The tri-hydroxyl-substituted compound (I) is found in several plants, *e.g.* *Morus alba* (Asano *et al.*, 1994), *Arachniodes standishii* (Furukawa *et al.*, 1985), *Angylocalyx boutiqueanus* (Nash *et al.*, 1985a), *Hyacinthoides non-scripta* (Watson *et al.*, 1997) among others, whereas the di-hydroxyl substituted compound (II) is found in the seeds of *Castanospermum australe* (Nash *et al.*, 1985b).

In a search for an effective synthetic path, *e.g.* good yield, to obtain both (I) and (II), it was found that they could be prepared starting from a common epoxide intermediate (III), which in turn could be prepared (Garcia, 2008) from (IV) when subjected to a Prilezhaev epoxidation (Prilezhaev, 1909; Swern, 1949). Herein, the crystal and molecular structures of (III) are described, motivated by the desire to unambiguously establish the relative configuration of the stereogenic centres. A further evaluation of the supramolecular association has been undertaken by analysing the Hirshfeld surface of (III).





2. Structural commentary

The molecular structure of (III), Fig. 1, comprises a pyrrolidyl ring fused to an epoxide O1 atom giving rise to a locally (mirror) symmetric fused-ring system. The nitrogen atom is connected to an ethyl ester group, with the carbonyl-O2 atom orientated towards the ring-methylene group. The pyrrolidyl ring is substituted in a 2-position by the 4-methoxyphenyl group. The conformation of the pyrrolidyl ring is an envelope with atom N1 being the flap atom and occupying a position *syn* to the epoxide-O1 atom. The dihedral angle between the fused three- and five-membered rings is $78.53(10)^\circ$, indicating an

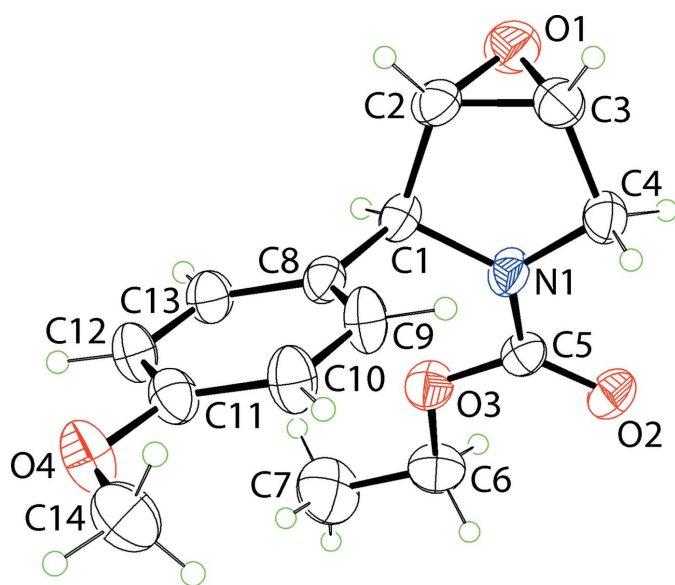


Figure 1

The molecular structure of (III), showing the atom-labelling scheme and displacement ellipsoids at the 35% probability level.

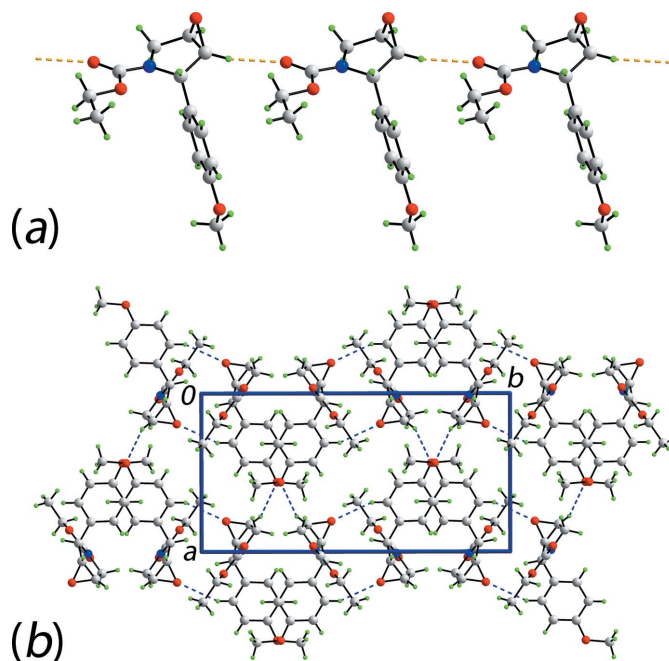


Figure 2

The molecular packing in (III): (a) a view of the supramolecular chain sustained by methine-C—H \cdots O(carbonyl) interactions shown as orange dashed lines and (b) a view of the unit-cell contents in projection down the *c* axis, whereby the chains illustrated in (a) are linked by weak benzene-C—H \cdots O(epoxide) and methine-C—H \cdots O(methoxy) contacts, shown as blue dashed lines.

almost orthogonal relationship. To a first approximation, the ethyl carboxylate group (r.m.s. deviation of the five non-hydrogen atoms = 0.0187 \AA) is planar and forms a dihedral angle of $17.23(9)^\circ$ with the five-membered ring. The 4-methoxyphenyl substituent is also approximately planar with an r.m.s. deviation of 0.0274 \AA for the eight fitted non-hydrogen atoms; the small twist of the methoxy group out of the plane of the benzene ring to which is connected, *i.e.* the C14—O4—C11—C12 torsion angle is $175.67(18)^\circ$, is primarily responsible for the deviations from exact planarity. The orthogonal relationship between this plane and that through the pyrrolidyl ring is seen in the dihedral angle formed between them of $85.02(6)^\circ$. Globally, the molecule has an extended planar region, comprising the pyrrolidyl ring and the ethyl ester residue with the epoxide O atom lying to one side of this plane and the 4-methoxyphenyl substituent to the other.

The chirality of each of the methine-C1—C3 atoms in the molecule illustrated in Fig. 1, is *S*, *S* and *R*, respectively, with the centrosymmetric unit cell containing equal amounts of both enantiomers.

3. Supramolecular features

The most prominent feature in the packing of (III) is the formation of a linear supramolecular chain sustained by methine-C—H \cdots O(carbonyl) interactions, as illustrated in Fig. 2*a*. The chains are aligned along the *c* axis and interactions between them are weak benzene-C—H \cdots O(epoxide) and

Table 1
Hydrogen-bond geometry (Å, °).

$D-H\cdots A$	$D-H$	$H\cdots A$	$D\cdots A$	$D-H\cdots A$
$C2-H2\cdots O2^i$	0.98	2.40	3.3559 (19)	165
$C13-H13\cdots O1^{ii}$	0.93	2.68	3.456 (2)	155
$C3-H3\cdots O4^{iii}$	0.98	2.68	3.311 (2)	107

Symmetry codes: (i) $x, y, z - 1$; (ii) $-x, -y + 1, -z$; (iii) $x - 1, y, z$.

methine- $C-H\cdots O$ (methoxy) contacts to sustain a three-dimensional architecture, Fig. 2*b*. Further insight into the molecular packing is provided by an analysis of the Hirshfeld surface below.

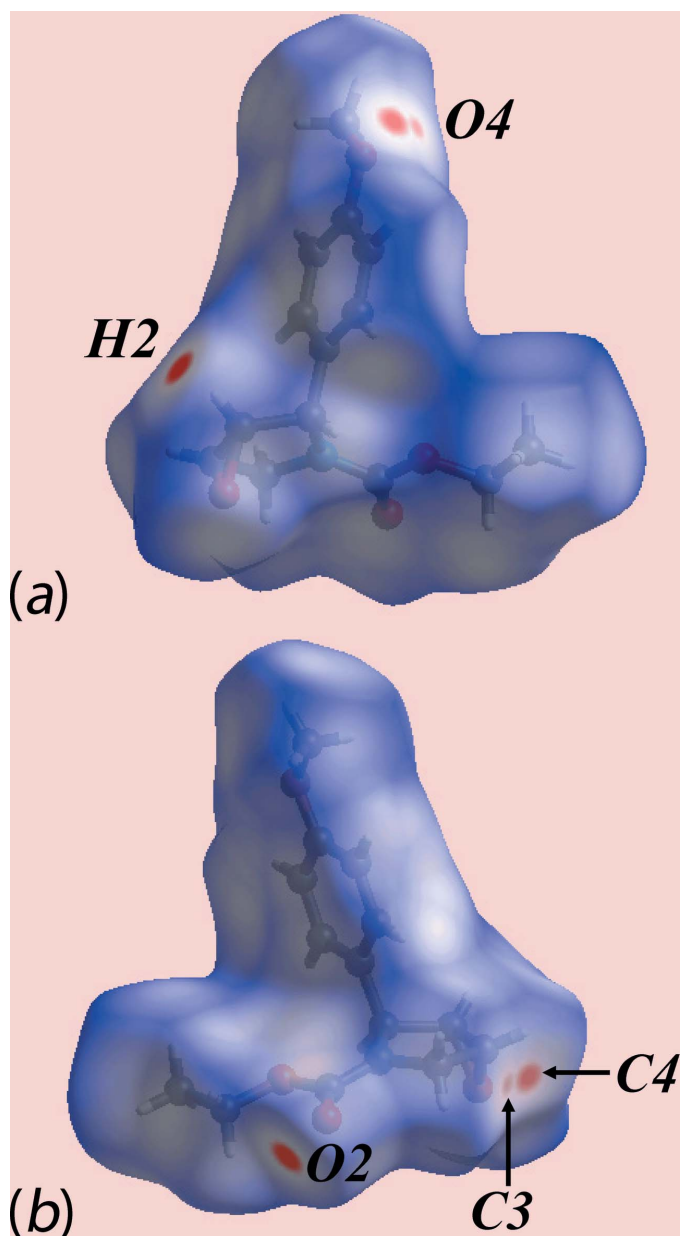


Figure 3
Two views of the Hirshfeld surface for (III) plotted over d_{norm} in the range -0.110 to 1.412 au.

Table 2
Summary of short inter-atomic contacts (Å) in (III).

Contact	Distance	Symmetry operation
$C4\cdots O4$	3.167 (2)	$-1 + x, y, z$
$O2\cdots H9$	2.63	$x, \frac{1}{2} - y, -\frac{1}{2} + z$
$C13\cdots H6A$	2.87	$x, y, -1 + z$

4. Hirshfeld surface analysis

The Hirshfeld surfaces calculated on the structure of (III) was conducted in accord with a recent publication (Zukerman-Schpector *et al.*, 2017) and provides more insight into the intermolecular interactions present in the crystal.

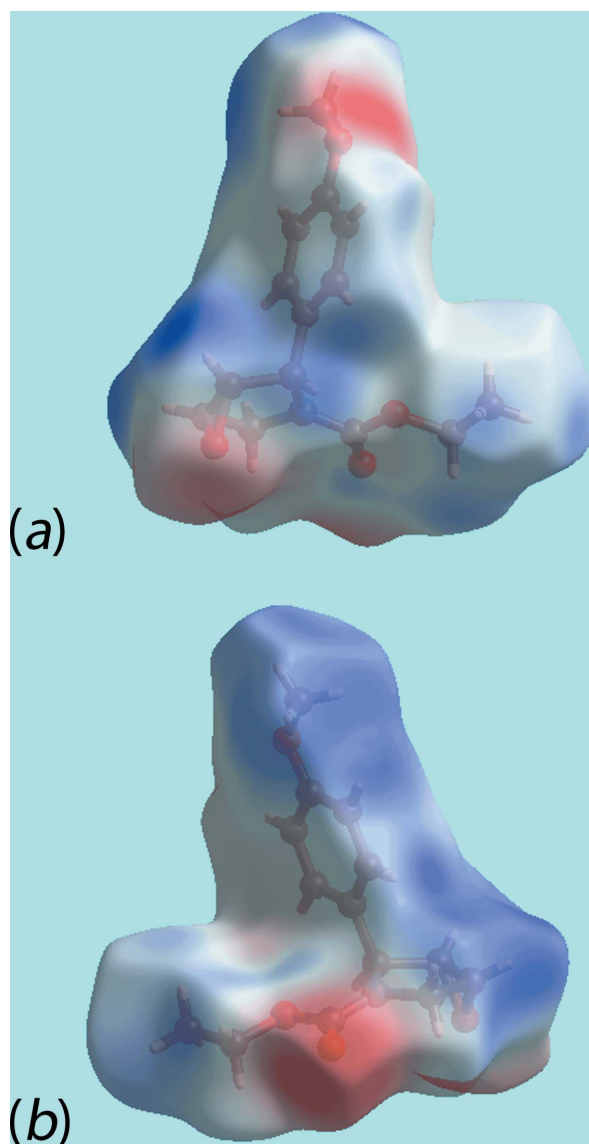


Figure 4
Two views of the Hirshfeld surface for (III) mapped over the calculated electrostatic potential in the range -0.083 to $+0.042$ au. The red and blue regions represent negative and positive electrostatic potentials, respectively.

The donor and acceptor of the C—H···O hydrogen bond instrumental for the formation of the supramolecular chain, *i.e.* between the methine-C—H2 and carboxylate-O2 atoms, are viewed as the bright-red spots near these atoms on the Hirshfeld surface mapped over d_{norm} in Fig. 3*a* and *b*. The bright-red spot, near methoxy-O4, and lighter spot, near methine-C3, and the diminutive red spot near methoxy-O4 and brighter spot near methylene-C4 in Fig. 3, are indicative of another C—H···O interaction (Table 1) and the short inter-atomic C···O/O···C contact (Table 2), respectively. On the Hirshfeld surface mapped over electrostatic potential in Fig. 4, the donors and acceptors of intermolecular interactions are represented by blue and red regions, respectively, corresponding to positive and negative electrostatic potentials near the respective atoms. The immediate environment about a reference molecule within Hirshfeld surfaces mapped over the electrostatic potential highlighting intermolecular C—H···O interactions and short inter-atomic O···H/H···O contacts (Table 2) is illustrated in Fig. 5.

The overall two dimensional fingerprint plot, Fig. 6*a*, and those delineated into H···H, O···H/H···O and C···H/H···C contacts (McKinnon *et al.*, 2007) are illustrated in Fig. 6*b–d*, respectively; the relative contributions from various contacts to the Hirshfeld surface are summarized in Table 3. The major contribution of 55.2% to the Hirshfeld surface is from inter-atomic H···H contacts, Fig. 6*b*, and is indicative of dispersive forces operating in the crystal. In the fingerprint plot delineated into O···H/H···O contacts, Fig. 6*c*, the 29.7% contribution results from the intermolecular C—H···O interactions and short inter-atomic O···H/H···O contacts, Tables 1 and 2. In the plot, Fig. 6*c*, a pair of spikes with their tips at $d_e + d_i \sim 2.4$ Å (with label '1') indicate the most significant C—

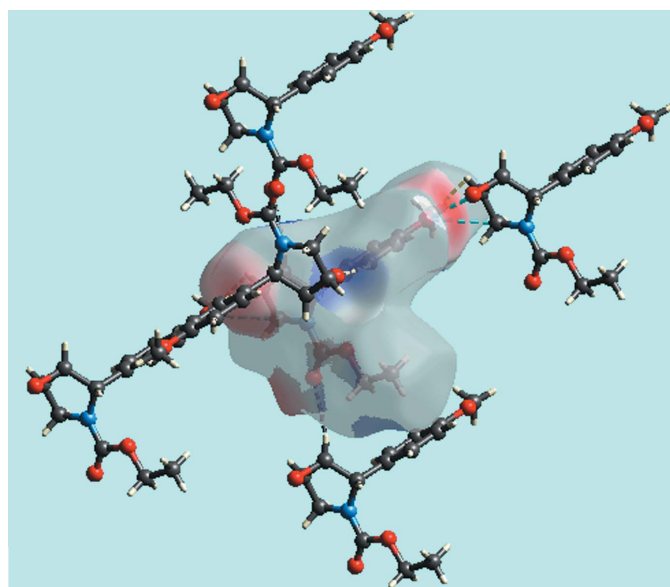


Figure 5

View of the Hirshfeld surface for (III) mapped over the electrostatic potential about a reference molecule showing C—H···O, C···O/O···C and short inter-atomic O···H/H···O contacts with black, sky-blue and white dashed lines, respectively.

Table 3

Percentage contributions of inter-atomic contacts to the Hirshfeld surfaces for (III).

Contact	Percentage contribution
H···H	55.2
O···H/H···O	29.7
C···H/H···C	13.0
C···C	1.1
N···H/H···N	0.5
C···O/O···C	0.4
O···O	0.1

H···O interaction whereas the pair of two adjoining parabola with their peaks at around $d_e + d_i \sim 2.7$ Å (label '2') represent short inter-atomic O···H/H···O contacts. The presence of the short inter-atomic C···H/H···C contact, Table 2, hitherto not mentioned, in Fig. 6*d*, leads to nearly symmetrical, characteristic wings with the pair of tips at $d_e + d_i \sim 2.9$ Å as highlighted with label '3'. The low contributions from other contacts, Table 3, have a negligible effect on the packing as their inter-atomic distances are greater than sum of their respective van der Waals radii.

5. Database survey

There are three structures in the crystallographic literature (Groom *et al.*, 2016) having the basic framework shown at the top of Scheme 2, *i.e.* with non-specific bonds between the atoms. Each of the three structures retrieved from the search, *i.e.* (V), (VI) (Csatayová *et al.*, 2015) and (VII) (Rives *et al.*,

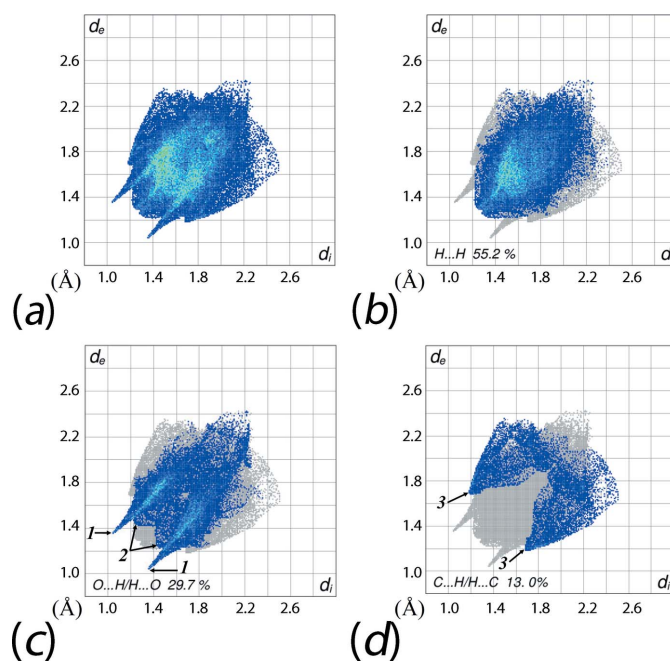
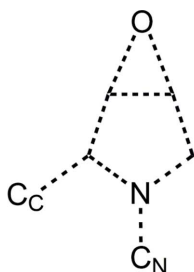


Figure 6

(a) The full two-dimensional fingerprint plot for (III) and fingerprint plots delineated into (b) H···H, (c) O···H/H···O and (d) C···H/H···C contacts.

2010) in Scheme 2, has the same bonds in the framework. The common feature of (V)–(VII) is an envelope conformation for the pyrrolidyl ring with the flap atom being the N atom which is *syn* to the epoxide O1 atom, *i.e.* as for (III). Major conformational differences are evident, however. With reference to the pyrrolidyl ring, in (V) and (VI), in common with (III), the ring-bound substituents occupy positions opposite to that of the epoxide O atom but, in (VII), this substituent lies to the same side of the pyrrolidyl ring.



Search protocol

- (V) $C_N = CH_2Ph$; $C_C = (CH_2)_{13}Me$
 (VI) $C_N = C(H)MePh$; $C_C = CH_2C(=O)O-tBu$
 (VII) $C_N = C(H)MePh$; $C_C = CH(OH)C(=O)O-tBu$

6. Synthesis and crystallization

The synthesis of (III) is as described in (Garcia, 2008). Crystals for the structure analysis were obtained by the slow evaporation of its $CHCl_3$ solution. M. p. 378–379 K.

7. Refinement details

Crystal data, data collection and structure refinement details are summarized in Table 4. The carbon-bound H atoms were placed in calculated positions ($C-H = 0.93-0.98 \text{ \AA}$) and were included in the refinement in the riding model approximation, with $U_{iso}(H)$ set to $1.2-1.5U_{equiv}(C)$.

Funding information

The support of the Brazilian agency, the National Council for Scientific and Technological Development (CNPq), for a fellowship to JZ-S (305626/2013–2) and a scholarship to FHS (121613/2016–0) is gratefully acknowledged.

References

Asano, N., Oseki, K., Tomioka, E., Kizu, H. & Matsui, K. (1994). *Carbohydr. Res.* **259**, 243–255.
 Blessing, R. H. (1995). *Acta Cryst.* **A51**, 33–38.
 Brandenburg, K. (2006). *DIAMOND*. Crystal Impact GbR, Bonn, Germany.
 Brás, N. F., Cerqueira, N. M. F. S. A., Ramos, M. J. & Fernandes, P. A. (2014). *Expert Opin. Ther. Pat.* **24**, 857–874.
 Burla, M. C., Caliandro, R., Carrozzini, B., Cascarano, G. L., Cuocci, C., Giacovazzo, C., Mallamo, M., Mazzone, A. & Polidori, G. (2015). *J. Appl. Cryst.* **48**, 306–309.

Table 4
Experimental details.

Crystal data	
Chemical formula	$C_{14}H_{17}NO_4$
M_r	263.28
Crystal system, space group	Monoclinic, $P2_1/c$
Temperature (K)	293
a, b, c (Å)	9.6467 (9), 18.408 (1), 7.8076 (6)
β (°)	102.071 (8)
V (Å ³)	1355.79 (18)
Z	4
Radiation type	Mo $K\alpha$
μ (mm ⁻¹)	0.10
Crystal size (mm)	0.30 × 0.27 × 0.11
Data collection	
Diffractometer	Enraf–Nonius TurboCAD-4
Absorption correction	ψ scan (Blessing, 1995)
T_{min}, T_{max}	0.933, 0.990
No. of measured, independent and observed [$I > 2\sigma(I)$] reflections	4187, 3927, 2107
R_{int}	0.028
$(\sin \theta/\lambda)_{max}$ (Å ⁻¹)	0.703
Refinement	
$R[F^2 > 2\sigma(F^2)], wR(F^2), S$	0.049, 0.147, 1.00
No. of reflections	3927
No. of parameters	174
H-atom treatment	H-atom parameters constrained
$\Delta\rho_{max}, \Delta\rho_{min}$ (e Å ⁻³)	0.17, -0.23

Computer programs: *CAD-4 EXPRESS* (Enraf–Nonius, 1989), *XCAD4* (Harms & Wocadlo, 1995), *SIR2014* (Burla *et al.*, 2015), *SHELXL2014* (Sheldrick, 2015), *ORTEP-3 for Windows* (Farrugia, 2012), *DIAMOND* (Brandenburg, 2006), *MarvinSketch* (ChemAxon, 2010) and *publCIF* (Westrip, 2010).

ChemAxon (2010). *Marvinsketch*. <http://www.chemaxon.com>.
 Csatajová, K., Davies, S. G., Figuccia, A. L. A., Fletcher, A. M., Ford, J. G., Lee, J. A., Roberts, P. M., Saward, B. G., Song, H. & Thomson, J. E. (2015). *Tetrahedron*, **71**, 9131–9142.
 Enraf–Nonius (1989). *CAD-4 EXPRESS*. Enraf–Nonius, Delft, The Netherlands.
 Farrugia, L. J. (2012). *J. Appl. Cryst.* **45**, 849–854.
 Furukawa, J., Okuda, S., Saito, K. & Hatanaka, S.-I. (1985). *Phytochemistry*, **24**, 593–594.
 Garcia, A. L. L. (2008). PhD thesis, Universidade Estadual de Campinas, UNICAMP, Campinas, SP, Brazil.
 Groom, C. R., Bruno, I. J., Lightfoot, M. P. & Ward, S. C. (2016). *Acta Cryst.* **B72**, 171–179.
 Harms, K. & Wocadlo, S. (1995). *XCAD4*. University of Marburg, Germany.
 McKinnon, J. J., Jayatilaka, D. & Spackman, M. A. (2007). *Chem. Commun.* pp. 3814.
 Nash, R. J., Bell, E. A., Fleet, G. W. J., Jones, R. H. & Williams, J. M. (1985b). *J. Chem. Soc. Chem. Commun.* pp. 738–740.
 Nash, R. J., Bell, E. A. & Williams, J. M. (1985a). *Phytochemistry*, **24**, 1620–1622.
 Prilezhaev, N. (1909). *Berichte*, **42**, 4811–4815.
 Rives, A., Ladeira, S., Levade, T., Andrieu-Abadie, N. & Génisson, Y. (2010). *J. Org. Chem.* **75**, 7920–7923.
 Sheldrick, G. M. (2015). *Acta Cryst.* **C71**, 3–8.
 Swern, D. (1949). *Chem. Rev.* **45**, 1–68.
 Watson, A. A., Nash, R. J., Wormald, M. R., Harvey, D. J., Dealler, S., Lees, E., Asano, N., Kizu, H., Kato, A., Griffiths, R. C., Cairns, A. J. & Fleet, G. W. J. (1997). *Phytochemistry*, **46**, 255–259.
 Westrip, S. P. (2010). *J. Appl. Cryst.* **43**, 920–925.
 Zukerman-Schpector, J., Prado, K. E., Name, L. L., Cella, R., Jotani, M. M. & Tiekink, E. R. T. (2017). *Acta Cryst.* **E73**, 918–924.

supporting information

Acta Cryst. (2017). E73, 1218-1222 [https://doi.org/10.1107/S2056989017009987]

Ethyl 2-(4-methoxyphenyl)-6-oxa-3-azabicyclo[3.1.0]hexane-3-carboxylate: crystal structure and Hirshfeld analysis

**Julio Zukerman-Schpector, Fabricia H. Sugiyama, Ariel L. L. Garcia, Carlos Roque D. Correia,
Mukesh M. Jotani and Edward R. T. Tiekink**

Computing details

Data collection: *CAD-4 EXPRESS* (Enraf–Nonius, 1989); cell refinement: *CAD-4 EXPRESS* (Enraf–Nonius, 1989); data reduction: *XCAD4* (Harms & Wocadlo, 1995); program(s) used to solve structure: *SIR2014* (Burla *et al.*, 2015); program(s) used to refine structure: *SHELXL2014* (Sheldrick, 2015); molecular graphics: *ORTEP-3 for Windows* (Farrugia, 2012) and *DIAMOND* (Brandenburg, 2006); software used to prepare material for publication: *MarvinSketch* (ChemAxon, 2010) and *pubCIF* (Westrip, 2010).

Ethyl 2-(4-methoxyphenyl)-6-oxa-3-azabicyclo[3.1.0]hexane-3-carboxylate

Crystal data

$C_{14}H_{17}NO_4$	$F(000) = 560$
$M_r = 263.28$	$D_x = 1.290 \text{ Mg m}^{-3}$
Monoclinic, $P2_1/c$	Mo $K\alpha$ radiation, $\lambda = 0.71073 \text{ \AA}$
$a = 9.6467 (9) \text{ \AA}$	Cell parameters from 25 reflections
$b = 18.408 (1) \text{ \AA}$	$\theta = 11.0\text{--}13.6^\circ$
$c = 7.8076 (6) \text{ \AA}$	$\mu = 0.10 \text{ mm}^{-1}$
$\beta = 102.071 (8)^\circ$	$T = 293 \text{ K}$
$V = 1355.79 (18) \text{ \AA}^3$	Irregular, colourless
$Z = 4$	$0.30 \times 0.27 \times 0.11 \text{ mm}$

Data collection

Enraf–Nonius TurboCAD-4 diffractometer	2107 reflections with $I > 2\sigma(I)$
non-profiled $\omega/2\tau$ scans	$R_{\text{int}} = 0.028$
Absorption correction: ψ scan (Blessing, 1995)	$\theta_{\text{max}} = 30.0^\circ$, $\theta_{\text{min}} = 2.2^\circ$
$T_{\text{min}} = 0.933$, $T_{\text{max}} = 0.990$	$h = -13 \rightarrow 13$
4187 measured reflections	$k = -25 \rightarrow 0$
3927 independent reflections	$l = -10 \rightarrow 0$
	3 standard reflections every 60 min
	intensity decay: 1%

Refinement

Refinement on F^2	174 parameters
Least-squares matrix: full	0 restraints
$R[F^2 > 2\sigma(F^2)] = 0.049$	Hydrogen site location: inferred from neighbouring sites
$wR(F^2) = 0.147$	H-atom parameters constrained
$S = 1.00$	
3927 reflections	

$$w = 1/[\sigma^2(F_o^2) + (0.0677P)^2 + 0.1423P]$$

where $P = (F_o^2 + 2F_c^2)/3$
 $(\Delta/\sigma)_{\max} < 0.001$

$$\Delta\rho_{\max} = 0.17 \text{ e } \text{\AA}^{-3}$$

$$\Delta\rho_{\min} = -0.23 \text{ e } \text{\AA}^{-3}$$

Special details

Geometry. All esds (except the esd in the dihedral angle between two l.s. planes) are estimated using the full covariance matrix. The cell esds are taken into account individually in the estimation of esds in distances, angles and torsion angles; correlations between esds in cell parameters are only used when they are defined by crystal symmetry. An approximate (isotropic) treatment of cell esds is used for estimating esds involving l.s. planes.

Fractional atomic coordinates and isotropic or equivalent isotropic displacement parameters (\AA^2)

	<i>x</i>	<i>y</i>	<i>z</i>	$U_{\text{iso}}^*/U_{\text{eq}}$
O1	-0.19247 (14)	0.42020 (8)	-0.03045 (18)	0.0678 (4)
O2	-0.03454 (14)	0.36201 (7)	0.53678 (14)	0.0565 (3)
O3	0.13930 (13)	0.42869 (6)	0.45731 (15)	0.0544 (3)
O4	0.56099 (13)	0.25574 (8)	0.0389 (2)	0.0734 (4)
N1	-0.01106 (14)	0.36816 (7)	0.25447 (16)	0.0467 (3)
C1	0.05665 (17)	0.39804 (9)	0.1171 (2)	0.0456 (4)
H1	0.0760	0.4499	0.1378	0.055*
C2	-0.05889 (19)	0.38771 (10)	-0.0450 (2)	0.0518 (4)
H2	-0.0341	0.3834	-0.1601	0.062*
C3	-0.17188 (18)	0.34308 (11)	-0.0031 (2)	0.0548 (4)
H3	-0.2228	0.3085	-0.0893	0.066*
C4	-0.13558 (18)	0.32331 (10)	0.1864 (2)	0.0513 (4)
H4A	-0.2129	0.3349	0.2438	0.062*
H4B	-0.1134	0.2720	0.2019	0.062*
C5	0.02590 (17)	0.38465 (9)	0.4251 (2)	0.0438 (4)
C6	0.1888 (2)	0.45044 (11)	0.6374 (2)	0.0621 (5)
H6A	0.2115	0.4081	0.7119	0.075*
H6B	0.1163	0.4783	0.6776	0.075*
C7	0.3173 (3)	0.49553 (15)	0.6432 (4)	0.0945 (8)
H7A	0.3893	0.4668	0.6074	0.142*
H7B	0.3517	0.5128	0.7605	0.142*
H7C	0.2941	0.5362	0.5656	0.142*
C8	0.19086 (17)	0.35884 (9)	0.10017 (19)	0.0439 (4)
C9	0.19617 (19)	0.28404 (10)	0.0936 (3)	0.0601 (5)
H9	0.1162	0.2574	0.1031	0.072*
C10	0.31680 (19)	0.24737 (11)	0.0733 (3)	0.0605 (5)
H10	0.3177	0.1969	0.0697	0.073*
C11	0.43576 (17)	0.28635 (10)	0.0583 (2)	0.0528 (4)
C12	0.43222 (19)	0.36132 (10)	0.0623 (3)	0.0594 (5)
H12	0.5117	0.3878	0.0498	0.071*
C13	0.31168 (18)	0.39740 (10)	0.0846 (2)	0.0529 (4)
H13	0.3113	0.4479	0.0893	0.063*
C14	0.5733 (2)	0.17891 (12)	0.0463 (3)	0.0757 (6)
H14A	0.5536	0.1618	0.1548	0.114*
H14B	0.6678	0.1651	0.0388	0.114*
H14C	0.5069	0.1579	-0.0497	0.114*

Atomic displacement parameters (\AA^2)

	U^{11}	U^{22}	U^{33}	U^{12}	U^{13}	U^{23}
O1	0.0615 (8)	0.0775 (10)	0.0667 (8)	0.0171 (7)	0.0183 (6)	0.0127 (7)
O2	0.0670 (8)	0.0661 (8)	0.0413 (6)	-0.0002 (6)	0.0225 (5)	0.0039 (6)
O3	0.0607 (7)	0.0603 (7)	0.0425 (6)	-0.0093 (6)	0.0113 (5)	-0.0074 (5)
O4	0.0470 (7)	0.0723 (9)	0.1044 (11)	-0.0043 (7)	0.0235 (7)	-0.0145 (8)
N1	0.0513 (8)	0.0550 (8)	0.0367 (6)	-0.0106 (6)	0.0160 (5)	-0.0021 (6)
C1	0.0540 (9)	0.0467 (9)	0.0398 (8)	-0.0054 (7)	0.0184 (7)	0.0018 (7)
C2	0.0551 (10)	0.0630 (11)	0.0397 (8)	0.0063 (8)	0.0150 (7)	0.0046 (7)
C3	0.0493 (9)	0.0694 (12)	0.0464 (9)	0.0004 (8)	0.0111 (7)	-0.0061 (8)
C4	0.0492 (9)	0.0586 (10)	0.0490 (9)	-0.0081 (8)	0.0170 (7)	-0.0026 (8)
C5	0.0491 (9)	0.0430 (8)	0.0409 (8)	0.0047 (7)	0.0130 (7)	0.0008 (6)
C6	0.0721 (12)	0.0627 (12)	0.0483 (10)	-0.0001 (10)	0.0052 (9)	-0.0143 (9)
C7	0.0973 (19)	0.0905 (18)	0.0904 (17)	-0.0297 (14)	0.0075 (14)	-0.0280 (14)
C8	0.0470 (8)	0.0495 (9)	0.0368 (7)	-0.0076 (7)	0.0122 (6)	-0.0006 (7)
C9	0.0517 (10)	0.0525 (11)	0.0820 (13)	-0.0152 (8)	0.0277 (9)	-0.0069 (9)
C10	0.0560 (10)	0.0479 (10)	0.0829 (14)	-0.0100 (8)	0.0263 (9)	-0.0104 (9)
C11	0.0453 (9)	0.0609 (11)	0.0523 (9)	-0.0071 (8)	0.0103 (7)	-0.0104 (8)
C12	0.0443 (9)	0.0613 (11)	0.0734 (12)	-0.0166 (8)	0.0139 (8)	-0.0026 (9)
C13	0.0513 (10)	0.0486 (10)	0.0587 (10)	-0.0105 (8)	0.0111 (8)	0.0003 (8)
C14	0.0633 (12)	0.0743 (14)	0.0884 (15)	0.0086 (11)	0.0131 (11)	-0.0168 (12)

Geometric parameters (\AA , $^\circ$)

O1—C3	1.443 (2)	C6—C7	1.485 (3)
O1—C2	1.447 (2)	C6—H6A	0.9700
O2—C5	1.2189 (18)	C6—H6B	0.9700
O3—C5	1.342 (2)	C7—H7A	0.9600
O3—C6	1.444 (2)	C7—H7B	0.9600
O4—C11	1.370 (2)	C7—H7C	0.9600
O4—C14	1.419 (3)	C8—C9	1.379 (2)
N1—C5	1.340 (2)	C8—C13	1.391 (2)
N1—C4	1.463 (2)	C9—C10	1.383 (2)
N1—C1	1.4739 (19)	C9—H9	0.9300
C1—C8	1.512 (2)	C10—C11	1.379 (2)
C1—C2	1.514 (2)	C10—H10	0.9300
C1—H1	0.9800	C11—C12	1.381 (3)
C2—C3	1.456 (2)	C12—C13	1.381 (3)
C2—H2	0.9800	C12—H12	0.9300
C3—C4	1.493 (2)	C13—H13	0.9300
C3—H3	0.9800	C14—H14A	0.9600
C4—H4A	0.9700	C14—H14B	0.9600
C4—H4B	0.9700	C14—H14C	0.9600
C3—O1—C2	60.50 (11)	C7—C6—H6A	110.4
C5—O3—C6	116.11 (13)	O3—C6—H6B	110.4
C11—O4—C14	118.28 (15)	C7—C6—H6B	110.4

C5—N1—C4	121.09 (13)	H6A—C6—H6B	108.6
C5—N1—C1	124.94 (14)	C6—C7—H7A	109.5
C4—N1—C1	113.68 (12)	C6—C7—H7B	109.5
N1—C1—C8	113.79 (13)	H7A—C7—H7B	109.5
N1—C1—C2	101.59 (13)	C6—C7—H7C	109.5
C8—C1—C2	111.17 (13)	H7A—C7—H7C	109.5
N1—C1—H1	110.0	H7B—C7—H7C	109.5
C8—C1—H1	110.0	C9—C8—C13	117.89 (16)
C2—C1—H1	110.0	C9—C8—C1	121.25 (14)
O1—C2—C3	59.63 (11)	C13—C8—C1	120.82 (15)
O1—C2—C1	113.23 (14)	C8—C9—C10	122.02 (16)
C3—C2—C1	109.74 (14)	C8—C9—H9	119.0
O1—C2—H2	119.9	C10—C9—H9	119.0
C3—C2—H2	119.9	C11—C10—C9	119.40 (18)
C1—C2—H2	119.9	C11—C10—H10	120.3
O1—C3—C2	59.87 (11)	C9—C10—H10	120.3
O1—C3—C4	112.52 (15)	O4—C11—C10	124.34 (17)
C2—C3—C4	109.22 (14)	O4—C11—C12	116.11 (15)
O1—C3—H3	120.2	C10—C11—C12	119.55 (17)
C2—C3—H3	120.2	C11—C12—C13	120.58 (16)
C4—C3—H3	120.2	C11—C12—H12	119.7
N1—C4—C3	103.12 (13)	C13—C12—H12	119.7
N1—C4—H4A	111.1	C12—C13—C8	120.55 (17)
C3—C4—H4A	111.1	C12—C13—H13	119.7
N1—C4—H4B	111.1	C8—C13—H13	119.7
C3—C4—H4B	111.1	O4—C14—H14A	109.5
H4A—C4—H4B	109.1	O4—C14—H14B	109.5
O2—C5—N1	124.47 (16)	H14A—C14—H14B	109.5
O2—C5—O3	124.44 (15)	O4—C14—H14C	109.5
N1—C5—O3	111.09 (13)	H14A—C14—H14C	109.5
O3—C6—C7	106.77 (17)	H14B—C14—H14C	109.5
O3—C6—H6A	110.4		
C5—N1—C1—C8	83.1 (2)	C1—N1—C5—O3	-4.0 (2)
C4—N1—C1—C8	-103.11 (16)	C6—O3—C5—O2	-1.0 (2)
C5—N1—C1—C2	-157.38 (15)	C6—O3—C5—N1	179.79 (14)
C4—N1—C1—C2	16.45 (18)	C5—O3—C6—C7	177.42 (17)
C3—O1—C2—C1	-100.05 (16)	N1—C1—C8—C9	47.4 (2)
N1—C1—C2—O1	54.73 (17)	C2—C1—C8—C9	-66.5 (2)
C8—C1—C2—O1	176.13 (13)	N1—C1—C8—C13	-134.82 (15)
N1—C1—C2—C3	-9.78 (18)	C2—C1—C8—C13	111.22 (17)
C8—C1—C2—C3	111.62 (15)	C13—C8—C9—C10	0.4 (3)
C2—O1—C3—C4	99.87 (16)	C1—C8—C9—C10	178.17 (16)
C1—C2—C3—O1	105.99 (15)	C8—C9—C10—C11	-0.3 (3)
O1—C2—C3—C4	-105.47 (16)	C14—O4—C11—C10	-4.4 (3)
C1—C2—C3—C4	0.5 (2)	C14—O4—C11—C12	175.67 (18)
C5—N1—C4—C3	157.71 (15)	C9—C10—C11—O4	179.54 (18)
C1—N1—C4—C3	-16.38 (18)	C9—C10—C11—C12	-0.6 (3)

O1—C3—C4—N1	-55.38 (17)	O4—C11—C12—C13	-178.80 (16)
C2—C3—C4—N1	9.10 (19)	C10—C11—C12—C13	1.3 (3)
C4—N1—C5—O2	3.4 (3)	C11—C12—C13—C8	-1.2 (3)
C1—N1—C5—O2	176.78 (15)	C9—C8—C13—C12	0.4 (3)
C4—N1—C5—O3	-177.35 (14)	C1—C8—C13—C12	-177.45 (15)

Hydrogen-bond geometry (Å, °)

<i>D</i> —H \cdots <i>A</i>	<i>D</i> —H	H \cdots <i>A</i>	<i>D</i> \cdots <i>A</i>	<i>D</i> —H \cdots <i>A</i>
C2—H2 \cdots O2 ⁱ	0.98	2.40	3.3559 (19)	165
C13—H13 \cdots O1 ⁱⁱ	0.93	2.68	3.456 (2)	155
C3—H3 \cdots O4 ⁱⁱⁱ	0.98	2.68	3.311 (2)	107

Symmetry codes: (i) $x, y, z-1$; (ii) $-x, -y+1, -z$; (iii) $x-1, y, z$.